〈論 文〉

緩傾斜 方程式을 利用한 港內의 波高豫測
A Prediction Method of Wave Deformation in Harbors Using the Mild Slope Equation

崔 善 皓*, 朴 相 吉**
CHOI Seon Ho and PARK Sang Kil

Abstract Since major reason of disaster in coastal area is wave action, prediction of wave deformation is one of the most important problems to ocean engineers. Wave deformations are due to physical factors such as shoaling effect, reflection, diffraction, refraction, scattering and radiation etc. Recently, numerical models are widely utilizied to calculate wave deformation. In this study, the mild slope equation was used in calculating wave deformation which considers diffraction and refraction. In order to solve the governing equation, finite element method is introduced. Even though this method has some difficulties, it is proved to predict the wave deformation accurately even in complicated boundary conditions. To verify the validity of the numerical calculation, experiments were carried out in a model harbour of rectangular shape which has mild slope bottom. The results by F.E.M. are compared with those of both Lee's method and the experiment. The results of these three methods show reasonable agreement.

要 指：海岸에서 發生하는 災害의 큰 原因은 波浪作用에 起因되기 때문에 海洋 技術者는 正確한 波浪變形을 豫測하는 것이 매우 重要하다. 波浪變形의 主要因은 淺水效果, 反射, 回折, 屈折, 散亂, 放射等을 들 수 있다. 最近, 波浪變形에 대하여 數値모델이 利用되고 있다. 本 硏究는 屈折과 回折를 同時에 考慮할 수 있는 緩傾斜方程式을 이용하여 有限要素法으로 數値모델를 樹立했다. 이 方法은 複雜한 境界條件을 갖는 海岸에 正確한 波浪豫測을 할수있는 長點이 있지만 몇가지의 改善해야할 問題點도 있는 것으로 나타났다.
本 計算結果를 檢定하기위해 模型實驗을 實施했다. 緩傾斜 方程式을 有限要素法으로 計算한 計算값과 Lee의 方法(Helmholtz 方程式을 有限差分法으로 數値計算한 方法)으로 計算한 값, 그리고 實驗값과 比較한 결과 妥當性 있는 一致를 얻었다.

INTRODUCTION

Today, goods transportation by ship is rapidly increasing day by day with the economic development and the increasing export-import amount. Because the decision of harbour location has a great effect on urban area near the harbour, we have to choose the place not to prevent civic development. Also the harbour engineer should consider the harbour resonance in new harbour planning as well as improvement and enlargement of old harbours. In the past, harbours were constructed considering only harbour resonance. Today, harbour construction is not limited in the coast but reached to estu-

* 正會員, 釜山大學校 大學院 土木工學科 博士過程
** 正會員, 釜山大學校 工科大學 土木工學科 副敎授

ary zone. Estuary harbour is the best place that can accommodate the transportation of both land and water. For harbour planning in estuarial zone, the engineer should consider both wave action and influx of river water. The problems of estuary harbour are as follows : wave deformation by influx of river water, mutual interference of flow, collapse of waterway in bay by a flow of littoral transport etc. In order to solve these problems, it is important to intercept incident wave and to control influx of river water. It is common to define the harbour resonance by wave height because wave deformation has the greatest effect on harbour resonance. To predict wave height accurately in estuary harbour, a governing equation that include the effects of both diffraction and refraction should be introduced. These effects can be calculated with mild slope equation.

This kind of papers are presented frequently in domestic and foreign journal. The wave prediction methods considering refraction and defraction are well known to coastal engineers, and these have been verified in applicability and validity for field application. But the reflection effect should be considered when the coastal structure is built in the harbour. In case that the inflow of river water is blocked by the structure in estuary harbour, the reflection effect owing to the coastal structure plays important role in harbour resonance.

Therefore, in this study, the reflection ratio is considered in the prediction of harbour resonance. The reflection ratio was computed in relation with the incident angle. The prediction of wave deformation using finite element method is suggested.(BETTES : 1977, BEHRENDT : 1985) Numerical simulation is carried out in a rectangular shape model harbour. The results are compared with those of both Lee's method(LEE : 1970) and hydraulic experiment.

MILD SLOPE EQUATION

Let's suppose that the fluid is incompressible and it's motion is irrotational. The incidient wave has amplitude of linear harmonic, propagating on a gentle slope. The wave motion can be written by the mild slope equation(M.S.E.) as follows;.

$$\nabla\cdot(b\nabla\eta)+\omega^2c\eta=0, \qquad (1)$$

in which

$$b=gh\frac{\tanh kh}{kh}\ \frac{1}{2}\left[1+\frac{2kh}{\sinh 2kh}\right]=CC_g$$

$$c=\frac{1}{2}\left[1+\frac{2kh}{\sinh 2kh}\right]=\frac{C_g}{C}$$

$$\omega^2=gk\cdot\tanh kh$$

Where C and Cg are the celerity of progressive wave and group velocity of wave respectively; g is the acceleration of gravity, η is elevation of the surface, h is the depth of water; and k is the wave number.

BOUNDARY CONDITIONS

Since M.S.E. is an elliptic partial differential equation, we have to give boundary conditions to all the perimeters of the region of computation. As shown in Fig.1,we call the front of structure Γ_1 as a fixed boundry, and a finite distance from harbour mouth Γ_2 as an open boundary.

Open boundary Condition

It is a half infinite region from the harbour mouth to the open boundary in a comparatively simple line coast in shape, where the depth of outer area R is constant. In the outer area R, each element of incident wave, reflecting wave, scattering wave are supposed.

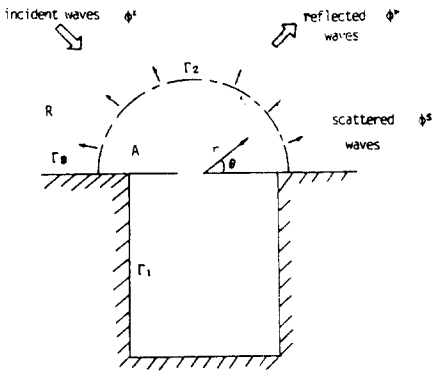

Fig. 1 Definition of boundaries

Velocity potential components ϕ^I, ϕ^r, ϕ^s, and the resultant velocity potential ϕ^R in area R may be written as follows;

$$\phi^R = \phi^I + \phi^r + \phi^s \tag{2}$$

$$\phi^I = -i\frac{g}{w} a^I e^{ikr\cos(\theta-\theta^I)} \tag{3}$$

$$\phi^r = -i\frac{g}{w} k_r a^I e^{ikr\cos(\theta+\theta^I)} \tag{4}$$

where a^I is the amplitude of the incident wave, θ^I, the incident angle, and k_r being the reflection ratio. The velocity potential of scattering wave ϕ^s satisfies the Sommerfeld's radiation condition as well as the Helmholtz equation, and may be represented by the following analytic series;

$$\phi^s = \sum_{n=0}^{\infty} H_n(k_r)[\alpha_n\cos(n\theta) + \beta_n\sin(n\theta) \tag{5}$$

in which α_n, β_n are unknown complex constants and H_n is the Hankel function of the first kind of order n.

Fixed boundary condition

We assume that both the incident wave and the reflection wave propagate sing in one direction. In Fig.1, the velocity potential in region A is ϕ^A ; velocity potential of incident wave and reflection wave is ϕ^I and ϕ^r respectively, we can get,

$$\phi^A = \phi^I + \phi^r \tag{6}$$

$$\phi^I = -ie^{ikr\cos(\theta-\theta^I)} \tag{7}$$

$$\phi^I = -iK_r e^{ikr\cos(\theta+\theta^I)} \tag{8}$$

The condition which is required on the fixed boundary states that

$$\frac{\partial\phi^A}{\partial y} = \frac{1}{r}\frac{\partial\phi^A}{\partial\theta} \quad \theta = 0\sim\pi \text{ on} \Gamma_1 \text{ and } \Gamma_3 \tag{9}$$

Computation of reflection ratio

By substituting Eqs.(6)−(8) into Eq.(9) and assuming that $k_x \ll k_y$, the reflection ratio may be calculated as

$$ik\frac{\partial\phi^A}{\partial y} + \alpha k^2\phi^A + \frac{\alpha}{2}\frac{\partial^2\phi}{\partial x^2} = 0 \tag{10}$$

Because Eq. (10) produces large error when the angle of incidence, θ^I approaches to zero, let's define α' as surface absorption rate for the connection of the angle of incidence and the reflection ratio as follows;

$$\alpha' = \frac{1-1/2(k_x/k)^2}{\sin\theta^I}\alpha = \frac{1+\sin^2\theta^I}{2\sin\theta^I}\alpha \tag{11}$$

Using the reflection ratio kr', we can expres s ' as follows;

$$\alpha' = \frac{1-K_r'}{1+K_r'} \tag{12}$$

$$K_r' = \frac{\alpha(1-\sin^2\theta^I)-2\sin\theta^I}{\alpha(1+\sin^2\theta^I)+2\sin\theta^I} \tag{13}$$

Or

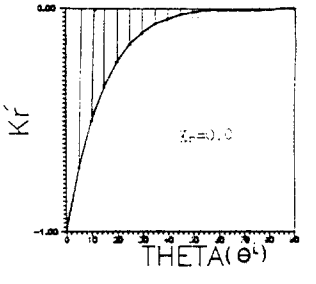

Fig.2 Relation Between K_r' and θ^I(K_r=0.0)

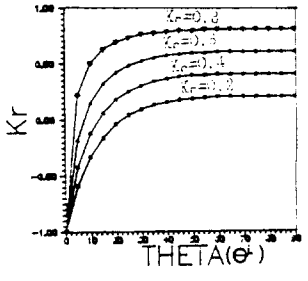

Fig.3 Relation Between K_r' and θ' (K_r=0.2, 0.4, 0.6, 0.8)

$$K_r'=\frac{(1-\sin\theta')^2-kr(1+\sin\theta')^2}{(1+\sin\theta')^2-kr(1+\sin\theta')^2} \quad (14)$$

Fig.2 expresses the relation between K_r' and θ' for K_r=0.0. The part of oblique line marked in the figure is the error caused by the approximation. Fig.3 shows the relation between K_r' and θ' for K_r= 0.2, 0.4, 0.6, 0.8.

Fig.2 and Fig.3 show the results of the computation in the fixed boundary condition. Error becomes smaller as the value of reflection ratio K_r increases. This means that the greatest error arises for K_r= 0.0 . There is no error in case of K_r= 0.0 even if θ' is greater than 60°. Also, in case of θ'=40°, the result shows good agreement.

DETERMINATION OF FUNCTIONAL

According to the assumption of M.S.E, $\Phi(x, y, z, t)$, the complex velocity potential and the complex amplitude can be written as Eq.(15), Eq.(16) respectively.

$$\Phi=\phi\frac{\cosh\ k(z+h)}{\cosh\ kh}\ e^{-iwt} \quad (15)$$

$$\eta=\frac{iw}{g}\ \phi \quad (16)$$

Total wave complex energy E per horizontal unit area is

$$E=\frac{\rho}{g}\ e^{-2iwt}\ \frac{1}{2}\ [CC_g(\nabla\phi)^2-\frac{C_g w^2}{C}\ \phi^2] \quad (17)$$

Complex energy flux E_f through the normal direction per hrizontal unit width is

$$E_f=\frac{\rho}{g}\ e^{-2iw}\ iwCC_g\phi\ \frac{\partial\phi}{\partial n} \quad (18)$$

The region of computatioion is divided into an inner region A and an outer region R. A boundary, ∂A lies on the bounday between A and B, and ∂R is an outer boundary of the region of computation. According to the conservation equation of total wave energy, a functional is acquired by

$$\frac{\partial}{\partial t}(E_A+E_R)+\int_{\partial B} E_f^A dS+\int_{\partial R} E_f^R dS=0 \quad (19)$$

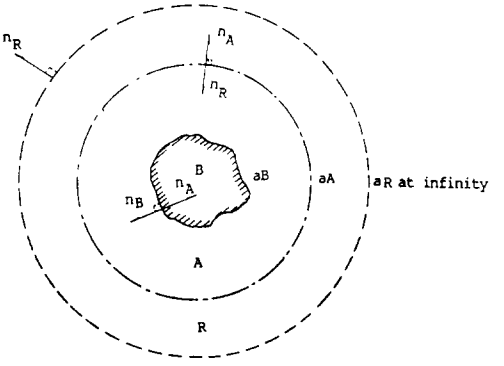

Fig. 4 Region of Computation

in which E_A and E_R are the complex wave energy of the region A and B respectively. E_f^A and E_f^R are the complex wave energy flux through the boundary B and ∂R, and ∂S being a line on the boundary ∂B and ∂R. The complex potential of the outer region R becomes.

$$E_R=\frac{\rho}{g}\ e^{-2iwt}\int_{\partial A+\partial B}\frac{1}{2}CC_g\phi_R\frac{\partial\phi_R}{\partial n_R}dS \quad (20)$$

So, functional $F(\phi)$ used in this study is given by

$$F(\phi)=\int\int_A \frac{1}{2}[CC_g(\nabla\phi)^2-\frac{C_g w^2}{C}\phi^2]dxdy$$
$$+\int_{\partial A} CC_g[\frac{1}{2}\phi^S(\phi_A-\phi)]\ \frac{\partial\phi_R}{\partial n_A}dS$$

$$-\int_{\partial A}\frac{1}{2}CC_k\phi^S\frac{\partial\phi}{\partial n_A}dS$$

$$\int_{\partial B}[\frac{1}{2}i\alpha wC_k\phi^2+\frac{i\alpha}{4k}CC_k(\frac{\partial\phi}{\partial S})^2]dS$$

$$=\text{const} \qquad (21)$$

DISCRETIZATION OF FUNCTIONAL

To make functional dimensionless, the representative length along the horizontal direction is taken as offshore wave length(L_o), while the representative length of a vertical direction is taken as the amplitude of the incident wave(a^I). The representative length of the time is used as the period(T). Because functional $F(\phi)$ has the dimension of m^6/s^4. Eq.(21) is multiplied by $[T/(L_o\ a^I)]\cdot(T/L_o)]^2$, to make it dimensionless as follows;

$$F(\phi)=\int\int_A\frac{1}{4}(1+G)[(\ell\nabla\phi)^2-(2\,\mathrm{II}\,\phi)^2]\,dxdy$$

$$+\int_{\partial A}\frac{1}{2}\ell^2(1+G)[\frac{1}{2}\phi^S-(\phi_A-\phi^I)]\frac{\partial\phi_R}{\partial n_A}dS$$

$$-\int_{\partial A}\frac{1}{4}\ell^2(1+G)\phi^S\frac{\partial\phi^I}{\partial n_A}dS$$

$$\int_{\partial B}[\frac{\mathrm{II}}{2}i\ell(1+G)\alpha\phi^2+\frac{i}{16\,\mathrm{II}}\ell^3(1+G)\alpha(\frac{\partial\phi}{\partial S})^2]dS \qquad (22)$$

where, $\ell=L/L_o$ (L_o : wave length in offshore), and $G=2kh/\sinh 2kh$.

If each term of the dimensionless functinal $F(\phi)$ is discretized, we can get an algebraical equation given by

$$F(\phi)=\frac{1}{2}[P]^t[M][P]+\frac{1}{2}[C]^t[M_1][C]+\frac{1}{2}[P]^t[M_2][C]+\frac{1}{2}[C]^t[M_2]+[P]+[Q_3]^t[P]+[Q_4]^t[C] \qquad (23)$$

in which

$[M]$, $[M_1]$, $[M_2]$ are the element coefficient determinant, and $[Q_3]$,$[Q_4]$ being element free term vector.

In the Eq.(23),using the unknown vector $[P]$, $[C]$, the total unknown vector $[\phi]$ can be expressed as follows;

$$[\phi]=[[P],[C]] \qquad (24)$$

in which $[\phi]$ is a row vector having N elements, and $[Q]$ element free term vector is expressed by;

$$[Q]=[[Q_3],[Q_4]] \qquad (25)$$

Since $[Q]$ is row vector with N elements like $[\phi]$, the determinant$[K]$ has $N\times N$ elements.

According to the stationary condition and $[K]$'s symmetricity, we can derive following;

$$[K][\phi]+[Q]=[0] \qquad (26)$$

Eq.(26) is the algebraic equation we want to solve. The velocity potential at every nodal point are solved using Eq.(26).

THE CONDITION OF COMPUTATION IN APPLICABLE RANGE OF NUMERICAL ANALYSIS

To verify the result of the numerical solution, we established a rectangular model harbour of 600m in length and 180m in width as shown in Fig.5.

Waves in the harbour experience complete reflection on the quay, and the constant water depth is 15m. In a certain place where Lee's method has a exact solution, we will verify the validity of the present method. We computed two cases that a wave direction is 195°, 225°, 270° with periods 75sec, 250 sec. As shown in Fig.5, the computational area is divided into elements of 30m in both x, y directions with 324 total element numbers, 193 total nodal points, 12 open boundary element numbers and 48 closed boundary element numbers.

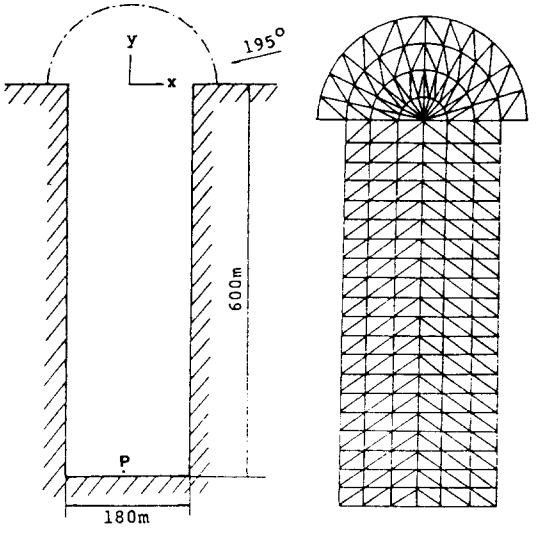

Fig. 5 Configuration of Model Harbor and Division of Finite Elememt

COMPARISON WITH LEE'S METHOD

Fig.6 shows a response curve at P location in Fig.5 when incidence angles are 195°, 225°, 270°. A vertical axis represents dimensionless value of the wave height divided by incident wave height at P location. A horizontal axis represents dimensionless values of the length of harbour multiplied by wave number k. The real line represents the results of computation by Lee's method while the dotted line represents the results of computation by finite element method. Three cases show that the results of both computations have good agreement. Also, the value of H/H_i shows peak values when $k\ell$ is 1.3 and 4.0.

If free oscillation is assumed to take place only in y direction of the model harbour, the undulation of period T can be obtained from

$$T=4\ell\,(1+4b/\pi\ell\,(0.9228+\ln(\pi b/2\ell\,)))^{1/2}/(gh)^{1/2} \quad (27)$$

In this case,the value of undulation period T_1, T_2, are 235.8 sec, 79.18sec in the first, second

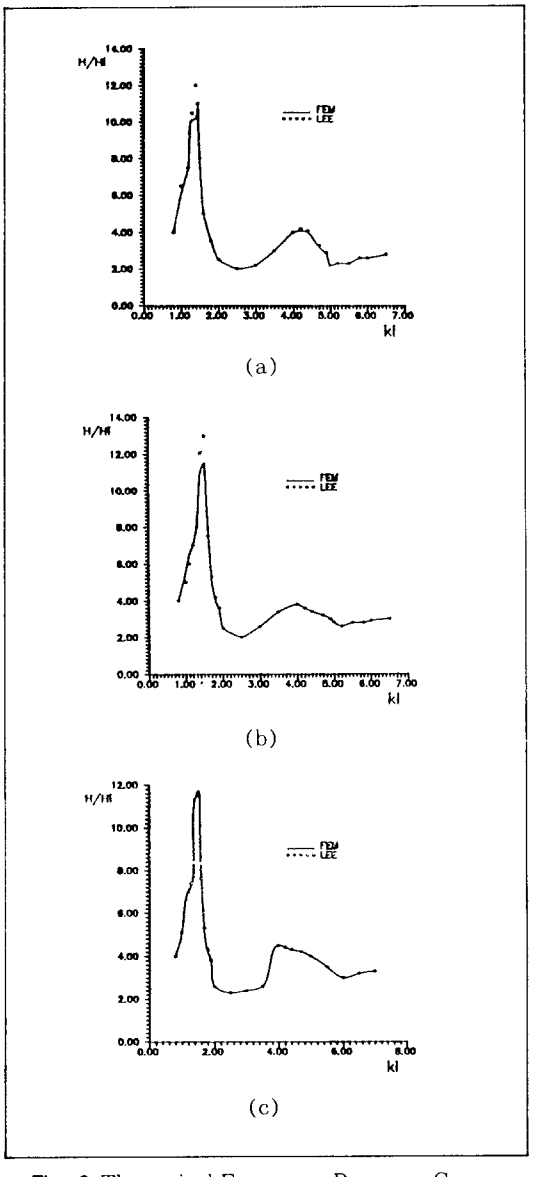

Fig. 6 Theoretical Frequency Response Curves (Lee's Method and F.E.M)

mode respectively. In these cases, $k\ell$ are 1.304 and 3.933, respectively, showing good agreement with the result of computation. The reason is that the length of harbour is long enough compared with the width of harbour entrance. According to the result, the value and location of peak show a little difference because the inci-

dence angle is different in the second mode. This means that the wave height increases as the incidence angle increases. In addition, the location of peak tends to move toward long periods(low frequency). This is because the oscillation of a harbour occurs hardly in the horizontal direction, but occurs in the vertical direction. As the incidence angle becomes smaller, the wave length of horizontal direction becomes shorter. Consequently, it can be concluded that the mathematical model of numerical analysis shows well the physical phenomenon of the response curve, and good agreement with Lee's method. Fig.7, (a), (b) indicate the distribution of wave height of both method for 195° in incidence angle of the incident wave. In Fig.7, the number means the value of dimensionless wave height.

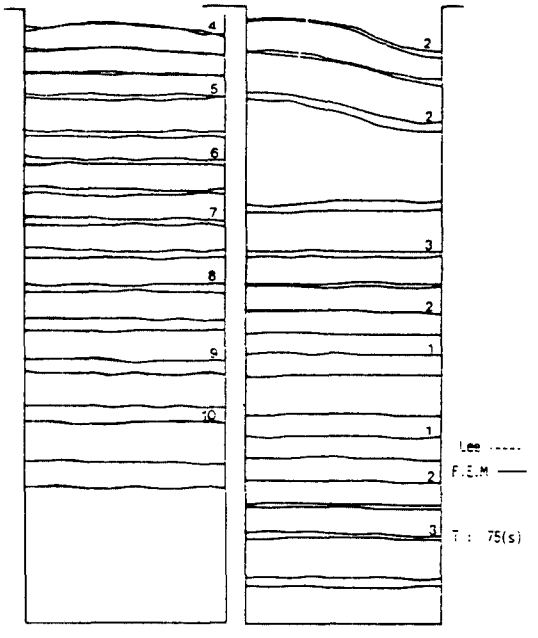

(a) (b)

Fig.7 Distribution of Wave Height in a Simple Harbour(Lee's Method and F.E.M)

The real line(FEM), the dotted line(Lee's method) are the result of each method. The first and second mode in T=250sec are shown in Fig.7 (a) and (b). Although these results show that a big difference is observed in node, it is very small compared with the length of the bay. Moreover, the one-fourth of the wave length in the first mode and the three-fourth of the wave length in te second mode in the bay, show well the physical phenomenon like a response curve. Both results show good agreement in quantity, proving that this model is suitable to predict the distribution of wave height for the case of constant depth and complete reflection.

HYDRAULIC EXPERIMENT

Outline of hydraulic experimentl

In order to compare and examine the distribution of computed wave height in the model harbour with experimental results, three dimensional hydraulic experiments were carried out. We used an outer plane water tank for experiment, having the length of 20m, the width of 5m and the height of 6m and equipped a flap type wavemaker at one end of the water tank. Rubbles were placed in both sides and the other end in front of the breakwater. The model harbour for three dimensional experiment are shown in Fig.8.

The incident waves have period T= 0.8, 0.9, 1.0, 1.5, 2.0 sec, with a constant wave height H_i =4.5cm. The angles of incident wave were 270° and 225°. The interval of wave height measurement was 5cm in the x, y direction, respectively. The depth of the harbour at the installation point of incident wave height profiler was 40cm, and the slope of bottom was kept one-tenth toward the shore.

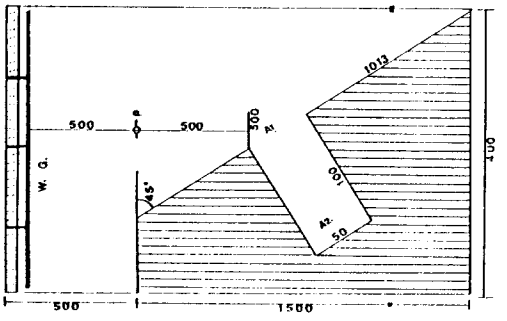

Fig. 8 Sketch of Wave Basin and Model Harbour

Distribution of wave height in longitudinal direction

Fig.9 is an example that shows the distribution of wave height. The vertical axis is the value of dimensionless wave height, the horizontal axis is the value of the length Y/ℓ. The real line represents the computed values. The black circles represent the experimented values in case that the angle of incident wave is 45°. The white circles are the experimented values in case that the angle of the incident wave is 90°. There are some discrepancies between the value of computation and that of theory. The reason is that the influence of the incidence wave was not considered exactly. On the other hand, the angle of the incident wave affects the distribution of wave height in the model harbour.

Fig.10 shows free-surface oscillation in the model harbour computed on the three dimen-

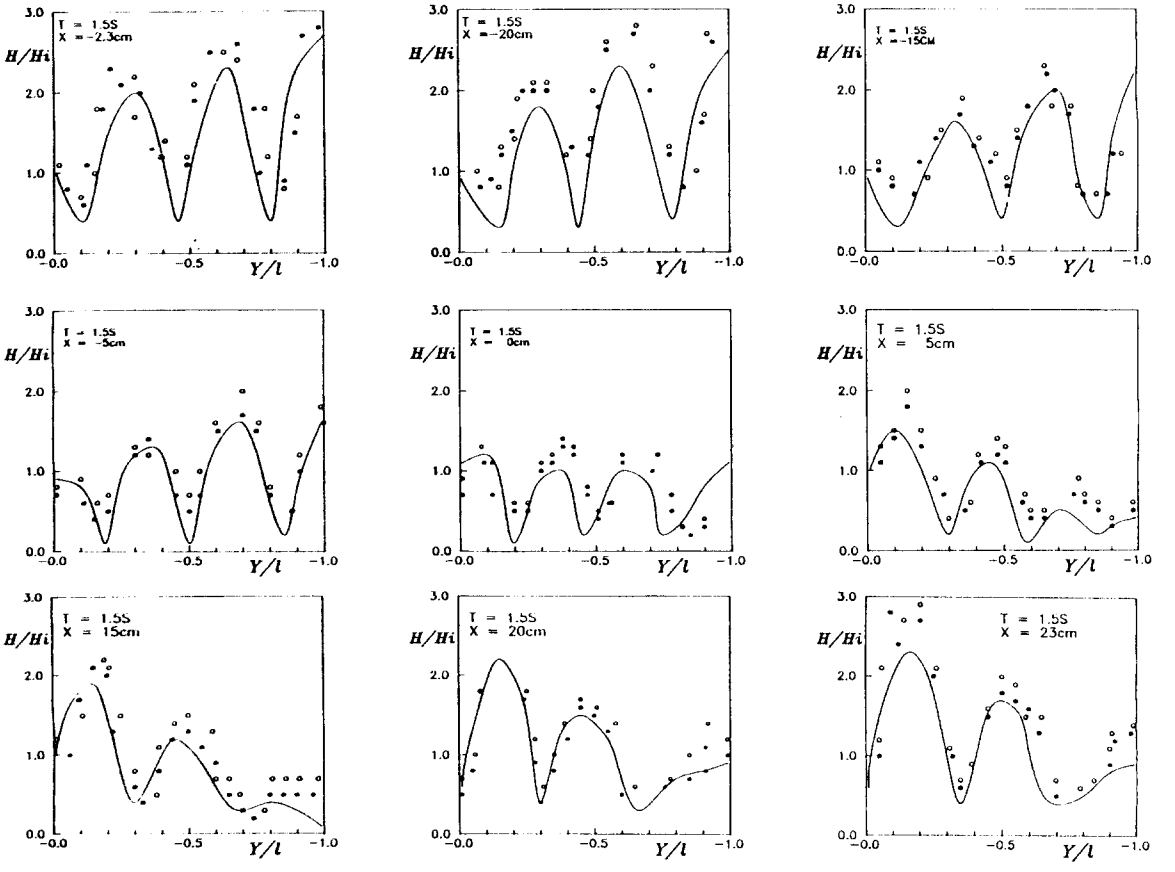

Fig. 9 Longitudinal Distribution of Wave Height in Model Harbour

sional plane. At the entrance of the harbour, the wave height is amplified more and more as transfer into the harbour. The peak value is shown in the middle of harbour. As time passed on, the of wave height decreases and the values of peak occur in front of the quay. The wave crest arises about at the point of L/4, because a standing wave is formed in the harour.

Distribution of wave height in cross-sectional direction

Fig.11 is one example that shows distribution of wave height in the harbour.

Fig.11 is used as the data for investigating swaying, heaving and rolling when a ship is anchored. The limit of wave height for safe unloading work is computed with the consideration of the influence on the unloading. The real line represents the computed value, the black circle represents the value experimented by Kubo in case that the angle of the incident wave is 45°, while the white circle represents the experimental value for the angle of the incident wave 90°. Some large differences are shown between the computed value and the experimented one. But the differences can decrease as the incidence angle is changed. The wave height distribution in horizontal direction show strong dependency on wave period T.

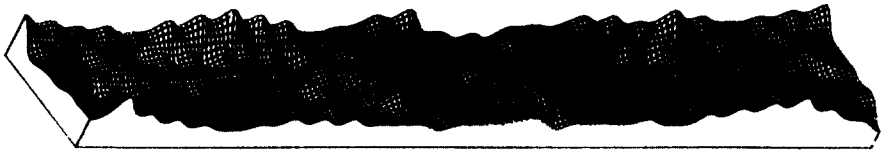

Fig. 10 Distribution of Wave Height in Model Harbour(Three Demension)

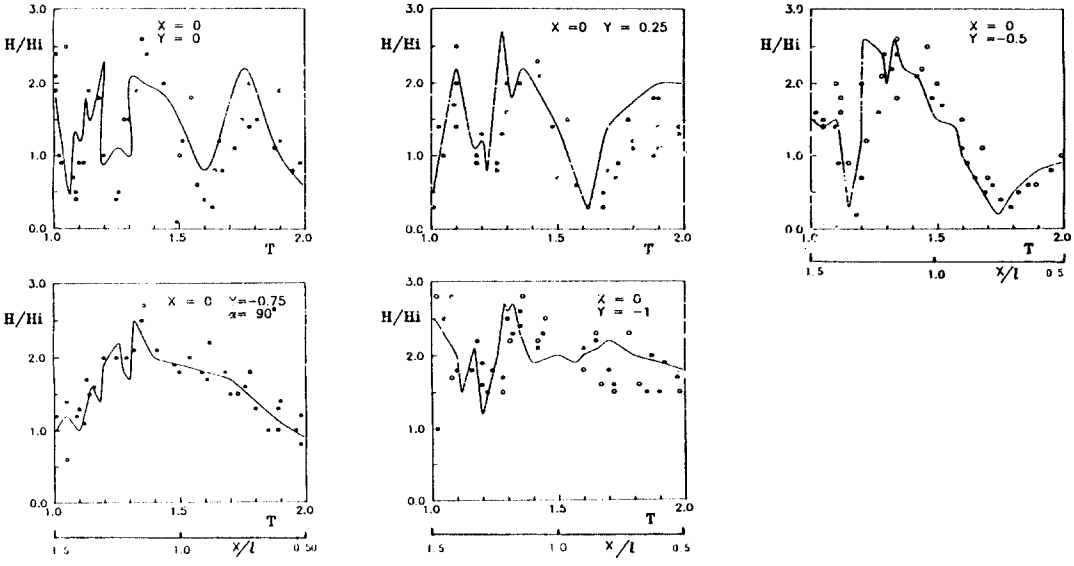

Fig. 11 The Cross Sectional Distribution of Wave Height in Model Harbour

CONCLUSIONS

Wave deformation in a model harbour was computed introducing finite element method with mild slope equation. A good agreement was found when compared with Lee's method by finite difference method. In addition, the hydraulic experiment was conducted to verify the results of computation. The experimental results give higher values than those of computation. The reason is that the influence of the incident wave was not considered enough. But the proposed numerical method are proved to predict harbour resonance reasonablely. The limit of computation region, computing time and troublesomeness of input information may be the subjects for further studies.

ACKNOWLEDGMENT

This paper was supported by NON-DIRECTED RESEARCH FUND, offered by the Korea Research Foundation, in 1989. 8-1991. 7

REFERENCE

1) BEHRENDT L.(1985) : A Finite Element Model for Water-Wave Diffraction Including Boundary Absorption and Bottom Friction, Paper 37, Institude of Hydrodynamics and Hydrulic Engineering, Technical Univ. of Demark.

2) BERKHOFF, J.C.W.(1976) : Mathematical Models for Simple Harmonic Linear Water Wave Diffraction and Refraction, Delft Hydraulics Laboratory, Holland, Publication No.163.

3) BETTES, P. and O.C. ZIENKIEWICZ(1977) : Diffraction and Refraction of Surface Wave Using Finite and Infinite Elements Int. Jour. For Numerical Methods in Engineering. Vol. 11, pp. 1271-1290. 4) ITO, Y. and TANIMOTE, K. (1972) : A Method of Numerical Analysis of Wave Propagation-Application of Wave Diffraction and Refraction, Proc. 13th., ASCE, pp. 503 -522.

5) KWAK, M.S., Hong, K.P. and Pyun, C.K. (1990) : Computation of wave height distribution inside a harbour using time-dependent mild slope equation, K.S.C.O.E. Vol.2 No.1, pp. 18-21.

6) LEE, J.J.(1970) : Wave Induced Oscillation in Harbour of Arbitrary Geometry, J. of Fluid Mechanics, Vol. 15 No. 2, pp. 375-394.

7) MARUYAMA, K. and KAJIMA, R.(1985) : Two Dimensional Wave Calculation Method Based on Unsteady Mild Slope Equations, Central Research Institude of Electric Power Industry, Japan Rep., No. 384041.

8) RADDER, A.C.(1979) : On the Parabolic Equation Method for Water Wave Propagation, J. of Fluid Mechanics, Vol. 95 No. 1 159-176.

9) SOUTHGATE, H.(1985) : A Harbour Ray Model of Wave Refraction-Diffraction, JWPCO, ASCE, Vol. 111 No. 1 pp. 29-43.

〈접수 : 6월 20일〉